



Supporting Online Material for

Maternal Alloantigens Promote the Development of Tolerogenic Fetal Regulatory T Cells in Utero

Jeff E. Mold, Jakob Michaëlsson, Trevor D. Burt, Marcus O. Muench, Karen P. Beckerman, Michael P. Busch, Tzong-Hae Lee, Douglas F. Nixon, Joseph M. McCune*

*To whom correspondence should be addressed. E-mail: mike.mccune@ucsf.edu

Published 5 December 2008, *Science* **322**, 1562 (2008)
DOI: 10.1126/science.1164511

This PDF file includes:

Materials and Methods
Figs. S1 to S9
References

Supporting Online Material

Supporting Online Material

Materials and Methods

Isolation and preparation of human tissues. All of the human tissue that was obtained for evaluation in this study was obtained with approval from and under the guidelines of the UCSF Committee on Human Research. Fetal tissues (mesenteric lymph node, spleen, and thymus) from 12-24 gestational week specimens and matched maternal blood samples were obtained from Advanced Bioscience Resources and San Francisco General Hospital. Infant thymus (7 months – 2 years) was obtained from normal donors undergoing thoracic surgery at Moffitt Hospital (University of California, San Francisco). Peripheral blood mononuclear cells (PBMCs) were isolated from healthy adults and children by density centrifugation over a ficoll-hypaque (Amersham Biosciences, Piscataway, NJ) gradient. Umbilical cord blood (UCB) was obtained in acid citrate dextrose or heparin sodium tubes by sterile cordocentesis. PBMCs from maternal and cord blood were isolated by ficoll-hypaque (Amersham Biosciences, Piscataway, NJ) gradient and cryopreserved using commercially-prepared freezing medium (IGEN; Origen, Inc., Gaithersburg, MD). Fetal lymph nodes, spleen, and thymus were processed as previously described (1). All tissues were extensively washed with sterile phosphate buffered saline (PBS) (> 40 mL per wash and > 5 washes per specimen) prior to harvesting cells. Whole fetal mesenteries were washed in PBS prior to isolation of individual LNs, which were scattered throughout the omentum. A typical fetal mesentery yielded 20-30 LNs and ~10-20 million mononuclear cells. Fetal spleen and thymus were processed by mechanical dispersion in sterile PBS (2% HI FBS) followed by incubation in 0.2 mg/ml collagenase B (Roche Diagnostics, Switzerland) for 1 hour at 37°C. In

some cases, red blood cells were removed by additional density centrifugation over a ficoll-hypaque gradient after collagenase digestion.

Analysis of maternal microchimerism. Detection of maternal microchimerism was performed as previously described (2-5). Briefly, whole cell suspensions were prepared from processed fetal tissues and from maternal blood samples, and cell pellets were frozen at ~3-5 million cells per tube. DNA was isolated from frozen cell pellets. Maternal and fetal HLA types (HLA-DR based assays) and insertion/deletion profiles (In/Del assay) were determined. Fetal samples were then analyzed for informative maternal alleles (i.e., maternal polymorphisms not present in the fetus) by quantitative allelespecific real-time polymerase chain reaction (qPCR) for the presence of minute amounts of maternal DNA. The fetal samples were also amplified by qPCR using primers specific to HLA-DQ alpha to determine the concentration of total DNA in each specimen. We estimated the concentration of total DNA and minor-type DNA (i.e., maternal cells) in the fetal samples by comparison of sample cycle thresholds to those from parallel amplification of 10-fold serial dilutions of standards with known cell count. We divided the concentration of maternal cell DNA by the concentration of total sample DNA to obtain the frequency of maternal cells in each fetal sample.

Cell preparation and antibody labeling. For flow cytometry analysis, cells were washed in flow cytometry staining buffer (PBS with 2% FBS and 2 mM EDTA) and incubated on ice in the presence of labeled antibodies for 45 minutes. Stained cells were then washed twice in MACS buffer and fixed in 2% paraformaldehyde. Antibodies used for phenotyping lymphocytes included: anti-CD3 Alexa Fluor 700 (SP34-2; BD Pharmingen, San Diego, CA), CD4 ECD (Clone T4; Beckman Coulter Inc. Fullerton, CA), CD8 PE-Cy5.5 (Clone 3B5; Caltag/Invitrogen, Carlsbad, CA), CD25 PE-Cy7

(Clone M-A251; BD Pharmingen), CD69 APC-Cy7 (Clone FN50; BD Pharmingen), and FoxP3 allophycocyanin (Clone PCH101; eBioscience, San Diego, CA). All cells were stained with a live/dead marker (Amine-Violet/Pacific Blue; Invitrogen) to exclude dead cells from the analysis. FoxP3 staining was carried out according to the manufacturer's protocol with slight modifications. Cells were washed twice in MACs buffer after staining with primary antibodies, re-suspended in FoxP3 fixation/permeabilization buffer (eBioscience), and then incubated for 1 hour at 4°C. Cells were washed twice in FoxP3 permeabilization buffer (eBioscience) and stained with FoxP3 APC in FoxP3 permeabilization buffer for 1 hour on ice. Cells were then washed 3 times in FoxP3 permeabilization buffer, and data were acquired with an LSRII flow cytometer (BD Biosciences, San Jose, CA) and analyzed with FlowJo software (Treestar, Ashland, OR).

Magnetic separation of cells. For *in vitro* assays involving cell depletion or selection, cells were washed in flow staining buffer and separated into different tubes based on selection criteria. For CD25 depletion/isolation, cells were incubated with anti-CD25 mAb directly conjugated to magnetic beads (Miltenyi CD25 Microbeads II) for 30-45 minutes at 4°C. Labeled cells were washed with flow staining buffer and run through magnetic columns (MS Columns, Miltenyi Biotec). The unbound fraction was kept as the CD25 negative (CD25-) fraction and the cells that were retained in the column were isolated later as the CD25 positive (CD25+) fraction, enriched in TReg. For mock depletions, cells were processed in parallel and incubated with anti-biotin magnetic beads (Miltenyi) and isolated following the same parameters (no flow through was collected). For APCs, whole PBMCs were incubated with biotin-conjugated anti-CD3 (BD Bioscience) and anti-CD56 (BD Bioscience) for 30 minutes on ice, and washed in flow staining buffer followed by incubation with anti-biotin magnetic beads (Miltenyi),

according to the manufacturer's protocol. Labeled cells were washed once more in flow staining buffer and passed over magnetic columns (MS columns). The flow-through was kept as APCs (CD3 and CD56 depleted, i.e., enriched for monocytes, B cells, macrophages, and dendritic cells). All cells purified by magnetic separation were monitored for purity by comparing them against unfractionated PBMCs using a standard phenotyping panel (listed above in *Cell preparation and antibody labeling*). Sorted cells were counted with a hemacytometer using trypan blue to determine the number of live cells, and re-suspended in appropriate buffer.

Mixed leukocyte reactions and in vitro proliferation assays with CFSE. For proliferation assays, cells were first labeled with the dye carboxy-fluorescein diacetate succinimidyl ester (CFSE) (Invitrogen). CFSE labeling was carried out by incubating cells in 1 μ M CFSE in PBS at 37°C for 10 minutes, followed by three washes in RPMI with 10% FBS. Labeled cells were added to 96-well U-bottom plates at a concentration of 300,000 cells/well in 200 μ l of RPMI culture media [10% HI FBS, 2 mM L-Glu, 100 U/mL penicillin/streptomycin (Invitrogen Life Sciences)]. For allogeneic/autologous MLRs, unlabeled APCs (CD3-CD56- lymphocytes) were irradiated (6000 rads from a cesium source) and 100,000 cells were added to wells for a final ratio of 1:3 (100,000 APCs per 300,000 responders). For all TReg add-back assays, 200,000 CFSE-labeled responder lymphocytes were incubated with a range of dilutions of CD25+ cells (positively-selected fraction) for 5 days. Stimulated cells were collected at various times and supernatants were stored for cytokine analysis. Cells were then washed in MACs buffer and prepared for flow cytometry analysis by incubation with appropriate antibodies. Typically, the same flow cytometry panel that was used for phenotyping [CD3 Alexa 700, CD4 ECD, CD8 PE-Cy5.5, CD25 PE-Cy7, CD69 APC-Cy7, and an

amine reactive dye (live/dead violet fixable dead cell stain kit (Invitrogen)) was used for CFSE assays. Unstimulated cultures were prepared in parallel and “background” levels of proliferation were measured and subtracted from final results. For *in vitro* MLRs where CFSE was not used (e.g., the kinetic experiment in Fig. 2), a similar set up was employed with the exception of the antibody panel used. For these experiments, anti-CD62L FITC was used in place of CFSE. Flow cytometry data were acquired on an LSRII and analyzed with FlowJo software.

Suppression assay with induced fetal TReg. Suppression assays for induced fetal TReg were performed as follows. Fetal mLN and spleens were obtained from 18-22 g.w. specimens. On day 0, fetal mLN were depleted of CD8⁺ T cells and CD25⁺ T cells by positive selection using miltenyi magnetic beads against CD8 and CD25. Fetal splenocytes were depleted of CD25⁺ cells by positive selection using miltenyi magnetic beads against CD25. All cells were taken for analysis of purity by flow cytometry to ensure appropriate depletion of indicated cell populations. Fetal CD25⁻ splenocytes were resuspended in freezing medium (90% HI FBS, 10% DMSO) on ice and stored in liquid N₂ during the primary stimulation of fetal CD8-CD25⁻ LN cells. Fetal CD8-CD25⁻ LN cells were stimulated with irradiated APCs from an unrelated donor in the presence or absence of a TGFβ inhibitor (SB-45312; 1μM) for 7 days. Fetal CD25⁺ splenocytes were cultured in parallel with recombinant human interleukin 2 (50U/mL) (added at days 0, 3, and 5). After 7 days in culture the stimulated fetal CD8-CD25⁻ LN cells and fetal CD25⁺ splenocytes were enumerated and monitored for FoxP3 expression by flow cytometry. Fetal CD25⁻ splenocytes were thawed, rested for >4 hours in fresh RPMI media (10% FBS, L-Glu, Pen/Strep) and counted using Trypan blue to determine cell death and yield after thawing. Fetal CD25⁻ splenocytes were then labeled with CFSE and cultured in 96-

well U-bottom plates at a concentration of 200,000 cells/well with 50,000 irradiated allogeneic APCs (same donor used to stimulate fetal LN cells). Pre-stimulated fetal CD8-CD25- LN cells and CD25+ splenocytes were added at different ratios and cultured with fetal CFSE+ CD25- splenocytes for 5 days. After 5 days proliferation was determined by flow cytometry (staining panel: CD3-Alexa 700, CD4-ECD, CD8-PE Cy5.5, CD25-PE Cy7, FoxP3-APC, Violet amine reactive live/dead marker-PB, and CFSE). Percent Suppression determined based on the following calculation: % Suppression = $1 - [(\%CFSE_{low} \text{ (total LN cells)}) / (\%CFSE_{low} \text{ (CD25-depleted)})] \times 100$. Statistical significance determined by unpaired Student's t-test.

Analysis of cytokine gene expression patterns in fetal and adult LNs. For adult LNs, total RNA was obtained from normal donors (26, 27, 29, 34 years old; all male) (Biochain, Hayward, CA). Fetal LNs (19-22 g.w.) were isolated as described above, and whole LNs were dispersed in lysis buffer (RNeasy kit Qiagen) and processed according to the manufacturer's protocol (Qiagen Inc. Valencia, CA). Cytokine gene expression patterns were determined by polymerase chain reaction (PCR)-based gene expression profiling of total adult and fetal LN RNA, using a pre-designed set of primers specific for a range of normal cytokines (General Cytokine Array, SuperArray Bioscience Corp. Frederick, MD). Preparation and analysis of samples was carried out according to the manufacturer's protocols. Briefly, total RNA concentration was measured, and RNA purity and integrity were verified using a bioanalyzer (Agilent Technologies, Santa Clara, CA). Reverse transcription was carried out to generate cDNA (SuperArray RT-PCR kit) and SYBR green-based quantitative real-time PCR was performed on samples (SuperArray, SYBR Green RT-PCR master mix). RT-PCR was run with an ABI 7700 (Applied Biosystems, Foster City, CA) and data were analyzed using a Microsoft Excel

platform designed by the manufacturer (SuperArray, General Cytokine Kit – Human).

Immunohistochemistry. Thymus sections were stained for FoxP3 as previously described (17). In brief, deparaffanized thymus sections from fetal and infant donors were incubated for 1 hour at room temperature with rabbit anti-FoxP3 (1:500 Ab #Ab10563, Abcam, Cambridge, MA). Detection was performed with the Dako Envision secondary detection system (Dako, Denmark), which employs a pre-diluted anti-rabbit antibody preparation that is directly conjugated to a horseradish peroxidase (HRP) polymer. 3,3'-diaminobenzidine (DAB) was used to develop slides, and images were acquired with a Leica DM 6000 microscope (Leica Microsystems, Wetzlar, Germany) and Image-Pro 5.1 software package (Media Cybernetics, Silver Springs, MD).

HLA Class I typing and immunophenotyping of umbilical cord blood (UCB) and maternal PBMC. Maternal and UCB PBMC were labeled with anti-HLA Class I haplotype-specific (A2/28, A3, A9, B8, B12, B13, B27, B57/58, Bw4, Bw6 and Class I positive control) mAbs (One Lambda Laboratories, Canoga Park, CA) that were directly fluorescein isothiocyanate (FITC)-conjugated by the manufacturer, conjugated with activated B-phycoerythrin (PE) using the Prozyme Phycolink B-Phycoerythrin Conjugation Kit (Prozyme, San Leandro CA), biotinylated, or unconjugated. Unlabeled primary mAbs were detected with allophycocyanin (APC)-conjugated goat anti-mouse IgG (Molecular Probes, Inc., Eugene, OR) and biotinylated antibodies were detected using streptavidin-APC (SA-APC) or streptavidin-PE (SA-PE). For more extensive immune phenotyping of maternal and fetal cells in UCB, FITC-conjugated mAbs directed against CD3, CD4, CD8, CD14, CD16, and CD19 were used in conjunction with PE or APC-labeled HLA antibodies. In all samples, propidium iodide (PI) was used as a marker of dead and dying cells. Flow cytometry was carried out on a FACSCan

(Becton Dickinson), and data were acquired using CellQuest software (Becton Dickinson) and analyzed using FlowJo software (Tree Star, Inc).

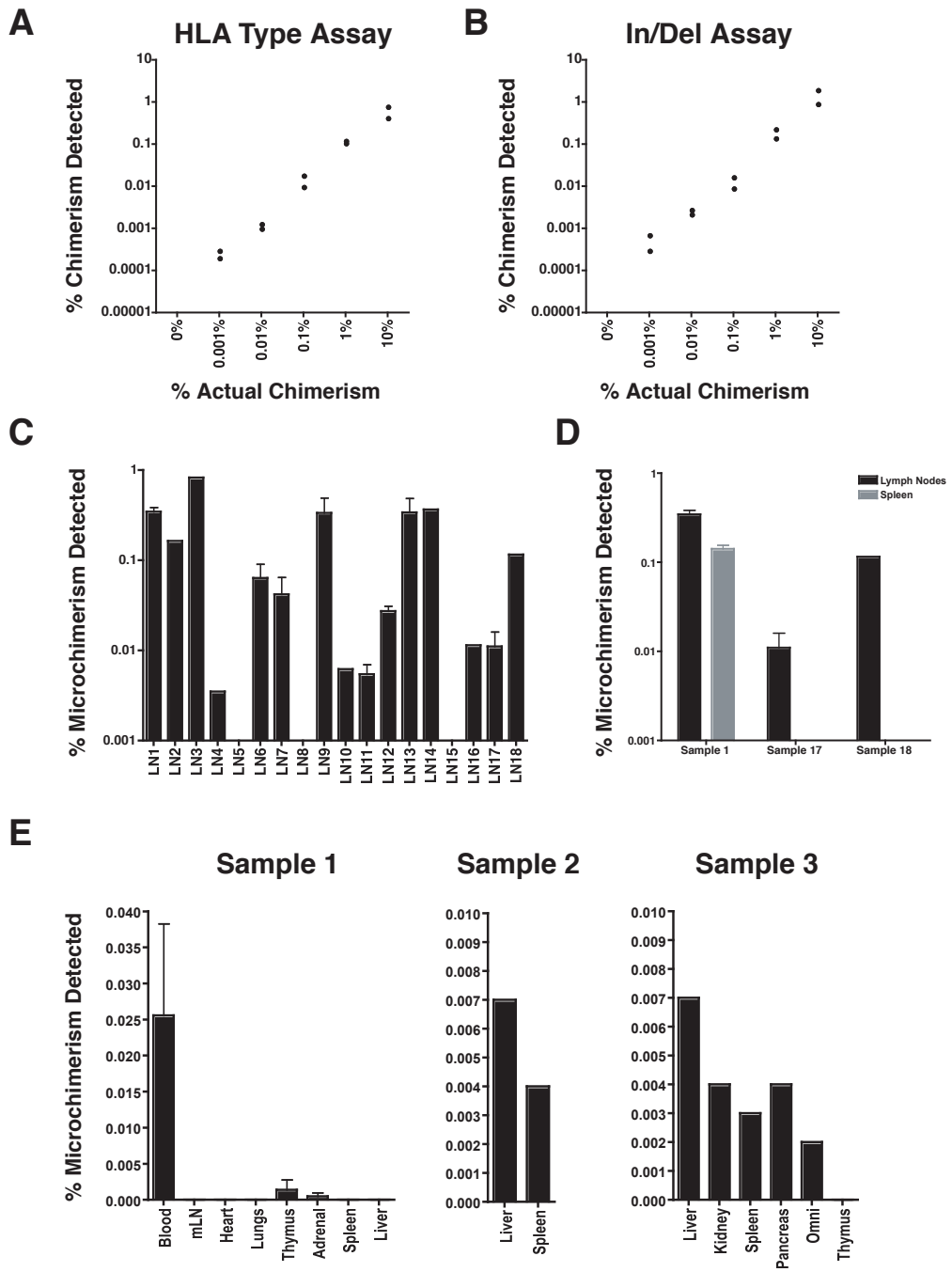
Sorting and genetic phenotyping of fetal and maternal populations in UCB. UCB samples were double labeled with FITC-labeled mAb directed against maternal HLA and a biotinylated mAb directed against the common fetal HLA, which was then detected with SA-APC or SA-PE. Labeled cells were incubated with PI and sorted on a FACSVantage cell sorter (Becton Dickinson). Cells identified as PI-negative (live), fetal HLA Class I negative, and maternal HLA Class I positive were collected, and assayed for the maternal HLA Class I allele by PCR, which was carried out using oligonucleotide primers specific for HLA-A2, -A3, -A9, -B8, and -B17 according to the manufacturer's instructions (One Lambda Laboratories). Briefly, cell lysate was mixed with commercially prepared and optimized PCR cocktail (D-mix; One Lambda Laboratories) and Taq-polymerase (Boehringer-Mannheim Laboratories) with standard cycling parameters in a GeneAmp PCR System 9700 (Applied Biosystems). PCR products were analyzed on a 5% agarose gel stained with ethidium bromide.

Supplemental References

1. J. Michaëlsson, J.E. Mold, J.M. McCune, D.F. Nixon, *J Immunol.* **176**, 5741 (2006).
2. T.H. Lee, D.M. Chafets, W. Reed, L. Wen, Y. Yang *et al.*, *Transfusion.* **46**, 1870 (2006).
3. W. Reed, T. H. Lee, P. J. Norris, G. H. Utter, M. P. Busch, *Semin Hematol.* **44**, 24-31 (2007).

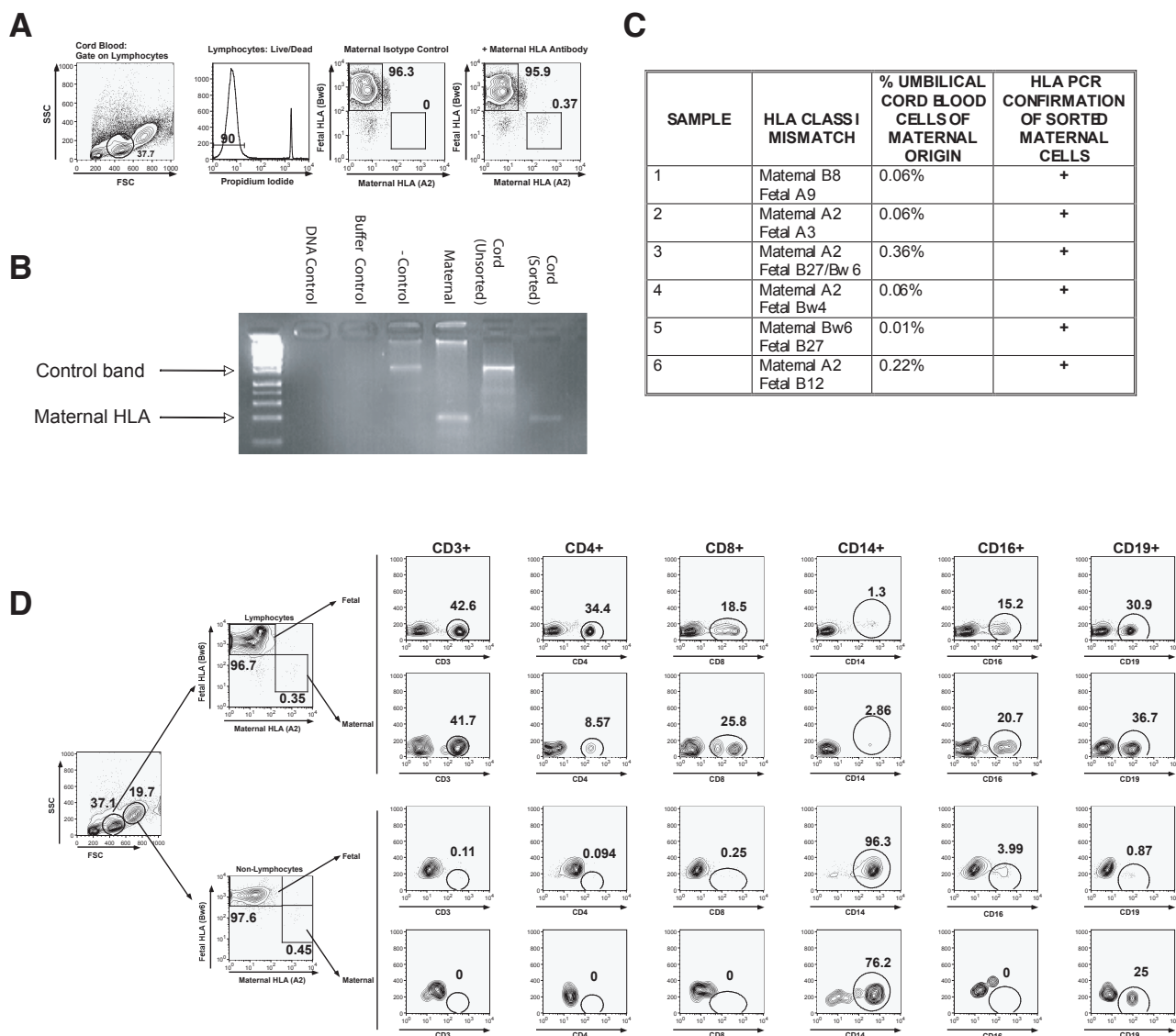
4. T. H. Lee, T. Paglieroni, G. H. Utter, D. Chafets, R. C. Gosselin *et al.*, *Transfusion*. **45**, 1280-90 (2005).
5. G. H. Utter, J. T. Owings, T. H. Lee, T. G. Paglieroni, W. F. Reed *et al.*, *J Trauma*. **58**, 925-32 (2005).
6. N. Watanabe, Y. H. Wang, H. K. Lee, T. Ito, Y. H. Wang *et al.*, *Nature*. **436**, 1181-85 (2005).

Fig. S1



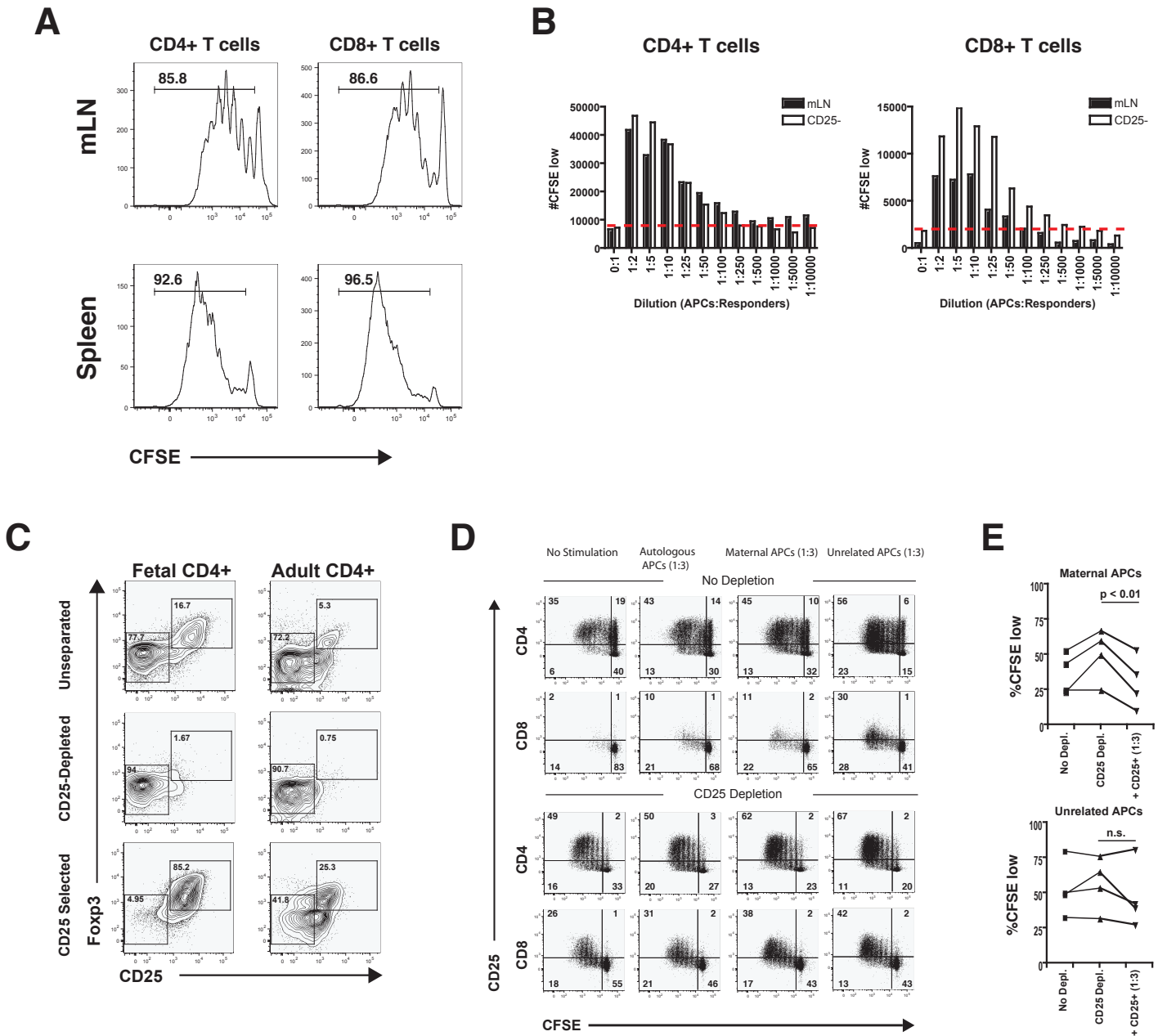
Supplementary figure 1. Detection of maternal microchimerism in the human fetus. Microchimerism assays were tested for accuracy by performing blinded experiments to detect the presence of chimerism in PBMCs (Donor A) spiked with PBMCs from an unrelated donor (Donor B) at concentrations ranging from 0.001% - 10%. Both (A) HLA-based and (B) Insertion/Deletion-based (In/Del) detection assays showed highly reproducible results. Note that both methods underestimate the actual level of chimerism, indicating that the actual level of microchimerism in the fetal samples may be higher. Points represent two separate samples of PBMCs from Donor A spiked with identical numbers of PBMCs from Donor B. Total numbers of cells used for testing microchimerism assays were consistent with the numbers of cells tested for fetal donors (~2-3 million cells). (C) Graphical representation of data from Table 1 in the main text (LN5 had no informative allele and LN8 and LN15 did not have detectable levels of chimerism). Error bars represent range of chimerism detected using HLA- or In/Del-based assays. (D) Analysis of maternal microchimerism in paired spleens and LNs from three donors. Only one spleen showed detectable levels of microchimerism, which was considerably lower than that detected in LNs. The LNs are less likely to come in contact with maternal cells during tissue harvesting since they are embedded in layers of connective tissue (omentum) within the mesentery. The experiment thus suggests that detection of microchimerism in LNs is not due to maternal contamination during the harvesting of the fetal tissues. (E) Organs from three intact products of conception were dissected and tested for the presence of maternal microchimerism. All three samples had detectable microchimerism, although only one was tested for chimerism in the LNs (which were negative). All three samples were very carefully processed to ensure that fetal tissues were not exposed to maternal cells during tissue harvesting. Blood analyzed in Sample 1 was obtained directly from the interior chamber of the heart.

Fig. S2

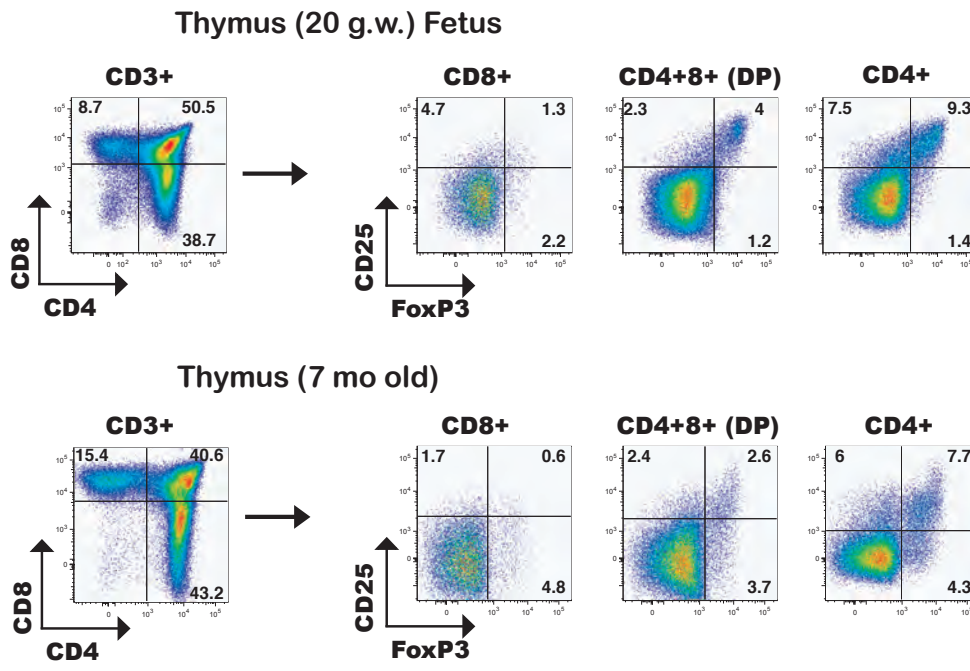
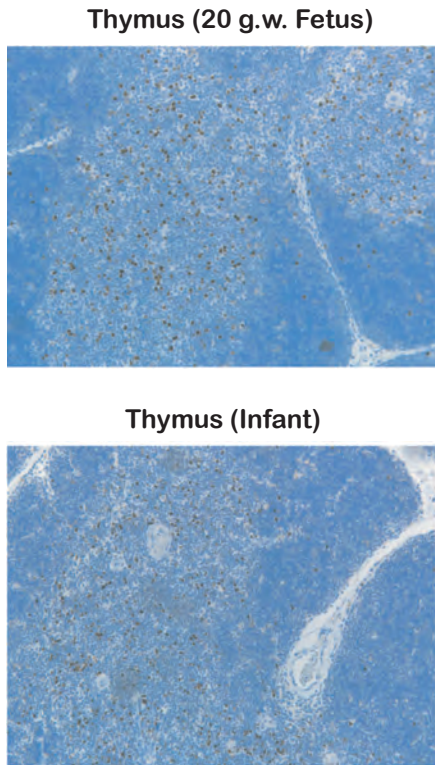
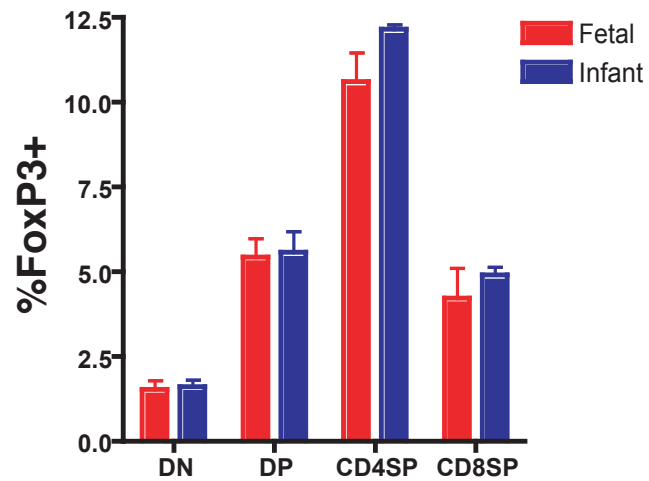


Supplementary figure 2. Maternal cells are present in full-term umbilical cord blood (UCB) and are represented by different lineages of immune cells. **(A)** Representative example of labeling and gating strategy used to detect unique non-inherited maternal- (HLA-A2 in this case) and paternally-inherited fetal (HLA-Bw6) HLA Class I types on the surface of UCB cells, including isotype control for maternal HLA Class I type to ensure specific staining. **(B)** The above strategy was used to sort and collect maternal cells from UCB, which were then lysed and analyzed for maternal HLA Class I alleles by PCR. A representative DNA gel is shown, demonstrating the presence of an appropriately-sized band representing amplification of the unique maternal allele which is present in maternal blood cells used as a positive control (Maternal) as well as in sorted maternal cells from UCB. The band was not detected in unsorted UCB, in DNA from cells known not to possess the maternal allele (- control), in PCR amplification reaction lacking added DNA (DNA control), or with lysis buffer added (Buffer control). **(C)** Summary table of six UCB samples tested detailing the percentage of live cells that were positive for maternal HLA Class I antigen and that were verified to be of unique maternal HLA Class I type by PCR. **(D)** Representative flow cytometry plots of fetal and maternal cells, demonstrating a different distribution of immune cells within these populations. Total cells were divided into lymphocyte and non-lymphocyte gates based on forward and side scatter characteristics to account for size and autofluorescence characteristics. As expected, CD14⁺ monocytes were found primarily in the non-lymphocyte gate, while most other cell types were detected in the lymphocyte gate, including cells positive for CD3, CD4, CD8, CD16 (likely predominantly NK cells), and CD19. Numbers in gates refer to percentage of the parent population that stained positively for a given marker.

Fig. S3

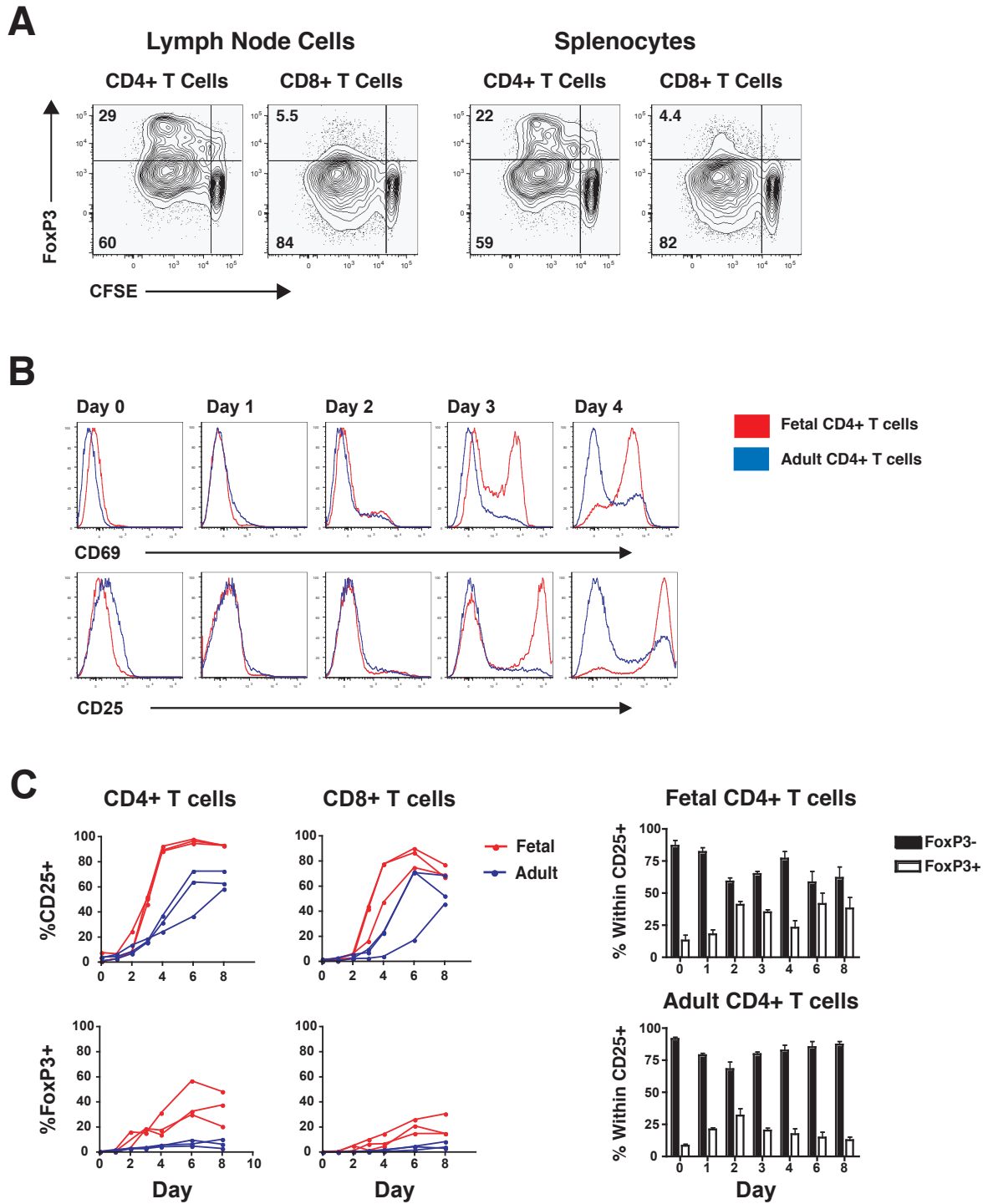


Supplementary figure 3. Fetal T cells from mLN and spleen are highly responsive to stimulation with alloantigens from unrelated donors. **(A)** Total lymphocytes from the spleen and mLN were isolated and stimulated in vitro with allogeneic APCs at a 3:1 ratio of fetal responders to allogeneic APCs. T cells from both LN and spleen were highly responsive to stimulation in primary MLRs (day 5) as measured by CFSE dilution. **(B)** To better illustrate the potential of fetal T cells to respond to alloantigens, fetal mLN cells were stimulated with allogeneic APCs from an unrelated donor at a range of dilutions. Proliferation was measured in terms of the number of cells that had divided. A substantial increase in the number of proliferating cells was observed at higher concentrations of allogeneic APCs and proliferative responses above background (0:1) were observed at ratios as low as 1:100. **(C)** Representative example of purities for fetal LNs or adult PBMCs after positive selection for CD25⁺ cells with magnetic beads. CD25 selection (and depletion) was efficient in fetal tissues due to the high expression of CD25 by fetal T_{Reg} and the absence of cells expressing intermediate levels of CD25 typically found in adult PBMCs (shown in the bottom right panel). **(D)** Proliferation of fetal CD4⁺ and CD8⁺ T cells after stimulation with different sources of APCs (no stimulation, autologous APCs, maternal APCs, or unrelated APCs), before (top) and after (bottom) depletion of CD25⁺ T_{Reg} cells. CD4⁺CD25⁺ T_{Reg} cells appear to proliferate in the undepleted LNs (top panels). After depletion of CD4⁺CD25⁺ T_{Reg} cells, responding CD4⁺CD25⁻ T cells were found to upregulate high levels of CD25. Removal of proliferating CD4⁺CD25⁺ T_{Reg} cells may lead to an underestimate of suppressed CD4⁺ T cells, as proliferating T_{Reg} cells are not observed after CD25 depletion. **(E)** Add-back of CD4⁺CD25⁺ T_{Reg} cells to cultures at a 1:3 ratio was found to suppress anti-maternal responses to a greater extent than unrelated APCs (n=4). Statistical significance was determined by paired Student's t-test.

Fig. S4**A****B****C**

Supplementary figure 4. Fetal and infant thymuses have comparable frequencies of FoxP3⁺ T cells. **(A)** Representative flow cytometry plots from a 20 g.w. fetal thymus and 7 month-old infant's thymus. All cells are gated on the CD3⁺ fraction to exclude immature thymocytes (which are predominantly FoxP3⁺). Similar frequencies of FoxP3⁺ cells are found in the 20 g.w. fetal thymus and in the infant's thymus, with the highest frequencies of FoxP3⁺ cells found in CD4SP thymocytes. **(B)** Immunohistochemistry of fetal and infant thymus for FoxP3⁺ cells. FoxP3⁺ cells are confined to the medullary region of both fetal and infant thymus, with rare cells present in the cortical regions. One significant difference regards the general absence of Hassall's corpuscles in the fetal thymus. Hassall's corpuscles begin to appear during fetal development and have been reported as early as 16 g.w. but are not prominent before 24 g.w. Recently, Hassall's corpuscles were reported to play a critical role in the generation of FoxP3⁺ T_{Reg} cells by secreting thymic stromal lymphoprotein (TSLP), leading to the activation of neighboring dendritic cells (6). Our findings that FoxP3⁺ medullary thymocytes are detectable at 12-14 g.w., before Hassall's corpuscles develop, and the relative consistency of FoxP3⁺ T cell frequency throughout development, argue that additional factors may contribute to FoxP3⁺ T_{Reg} development in the thymus. **(C)** The frequency of FoxP3⁺CD3⁺ T cells in fetal (n=5) and infant (n=2) thymuses was measured by flow cytometry. No difference was detected for any of the CD3⁺ thymocyte subsets.

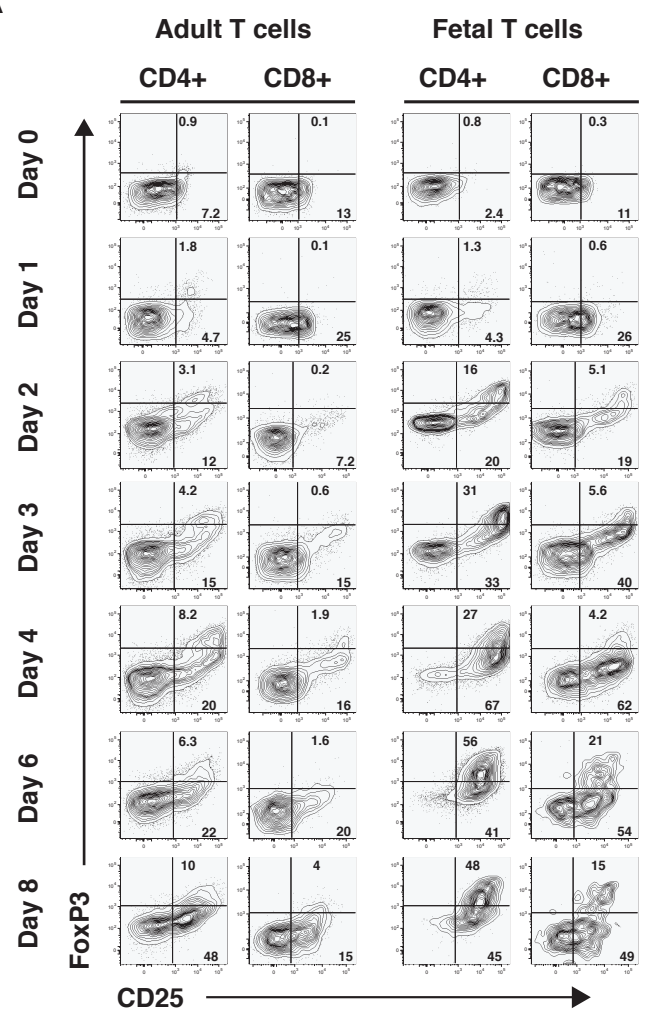
Fig. S5



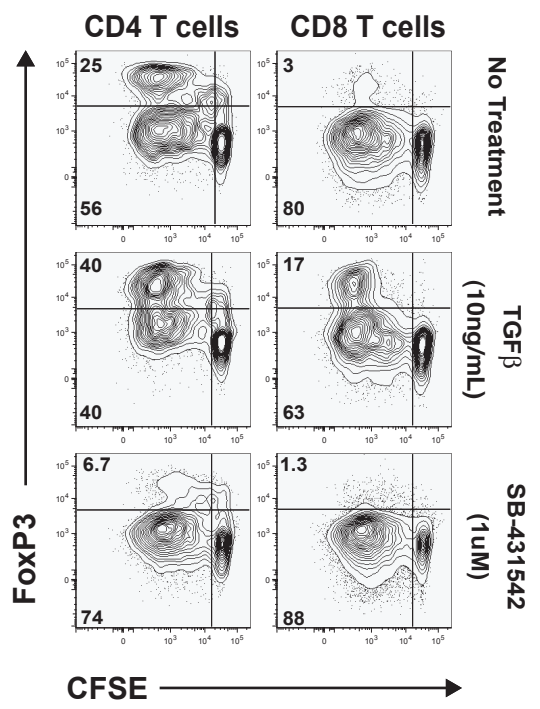
Supplementary figure 5. Upregulation of FoxP3 after stimulation of fetal T cells with allogeneic APCs. **(A)** Fetal LN cells and splenocytes were cultured with a single unrelated allogeneic donor in a 5-day MLR. FoxP3 expression was determined in CD4⁺ and CD8⁺ T cells in relation to proliferation (CFSE dilution). **(B)** Comparison of activation markers on fetal and adult CD4⁺ T cells after stimulation with allogeneic APCs. No differences were observed for fetal or adult CD4⁺ T cells in the first two days of a primary MLR. However, on the third day of stimulation, a massive expansion of CD69⁺CD25^{bright} cells was detected amongst the fetal T cells. After four days of stimulation, almost all fetal CD4⁺ T cells were CD69⁺CD25^{bright} whereas only a small fraction of adult T cells were CD69⁺CD25^{bright}. **(C)** Upregulation of CD25 and Foxp3 by fetal or adult T cells as a function of time (3 fetal and 3 adult donors are shown). Within the activated, CD25⁺ population of cells, there is a greater fraction of FoxP3⁺ cells in fetal vs adult CD4⁺ T cells.

Fig. S6

A

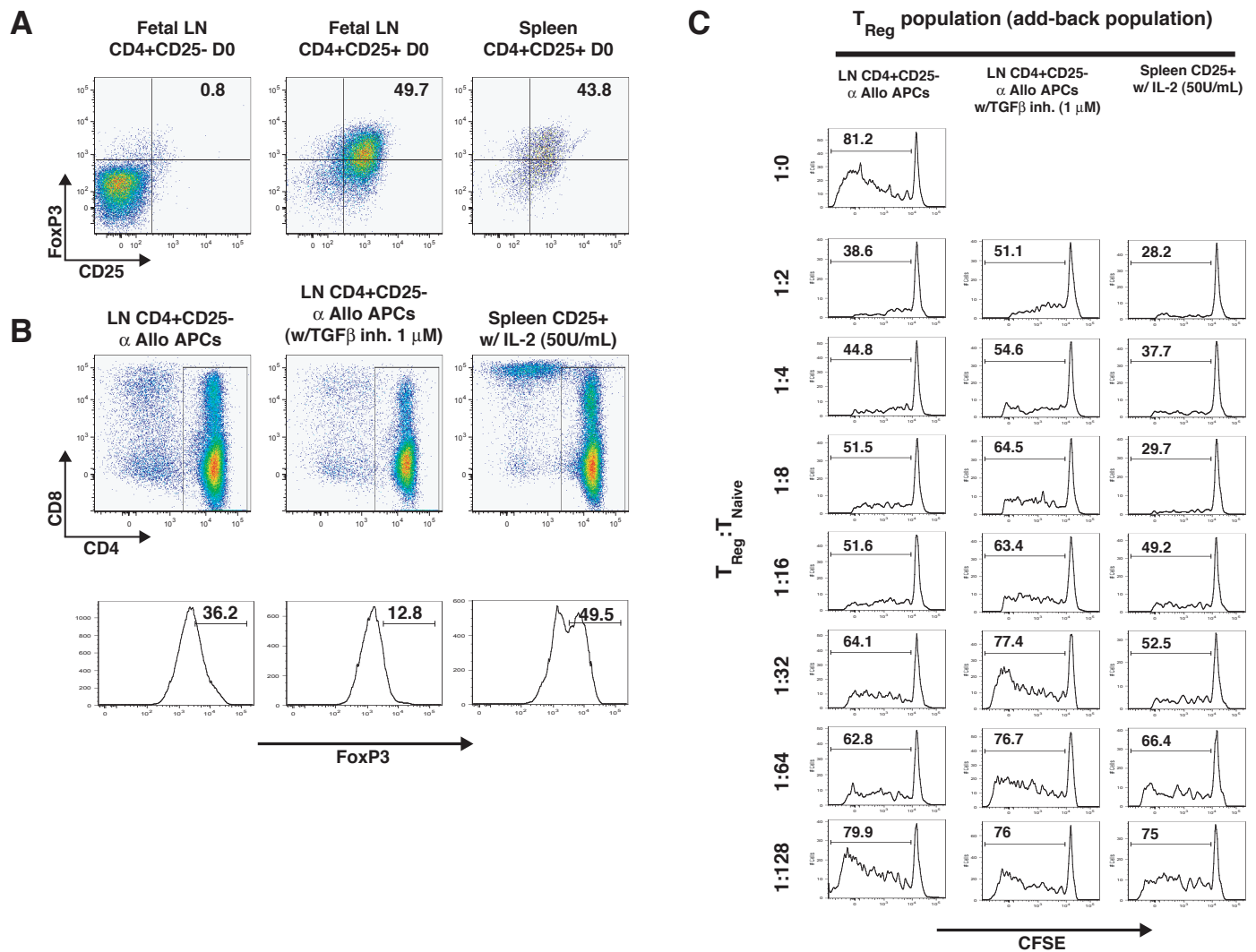


B

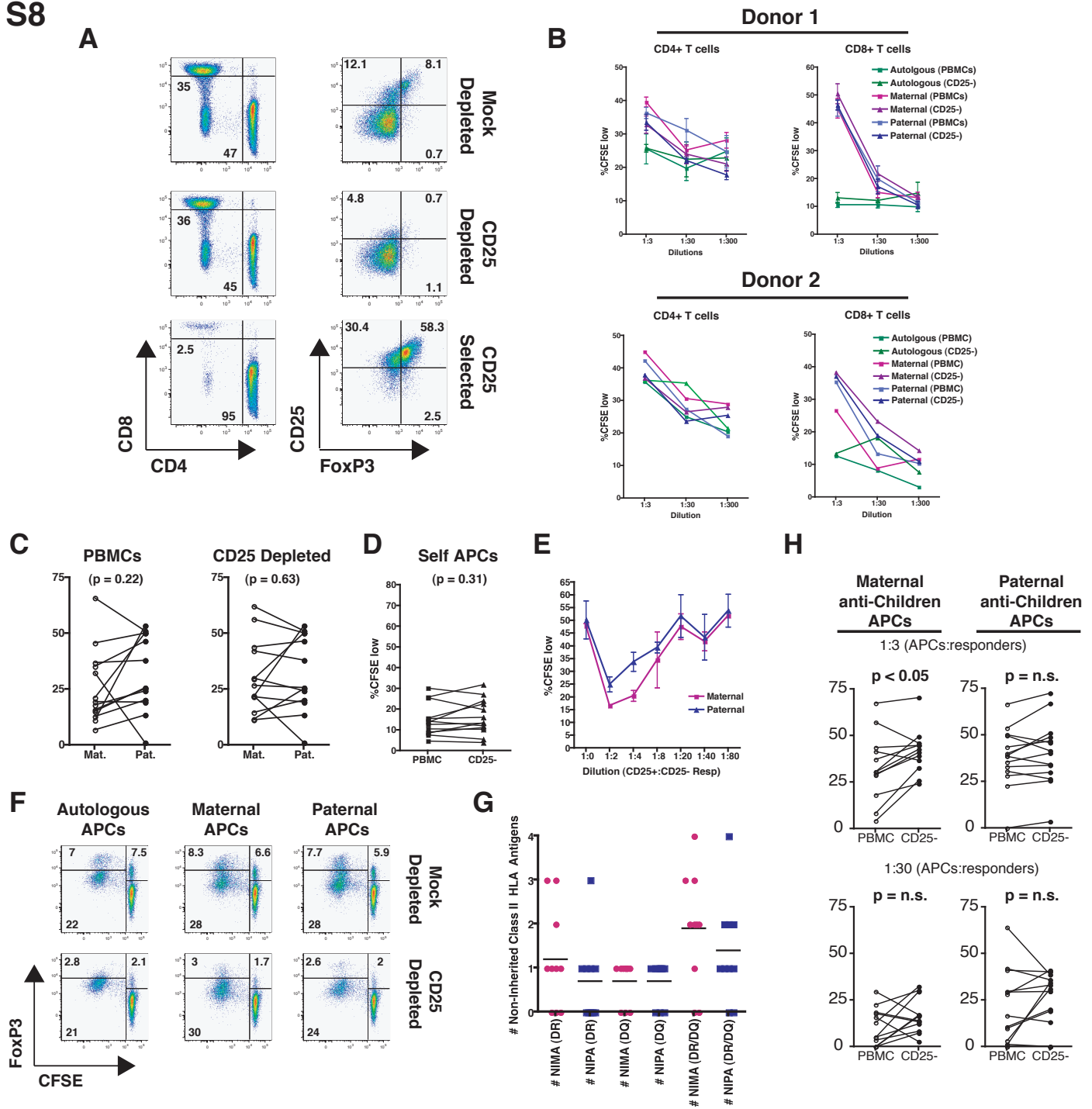


Supplementary figure 6. (A) Kinetic analysis of adult and fetal CD4⁺ and CD8⁺ T cell activation following stimulation with APCs from a single unrelated donor. CD25 and FoxP3 expression are shown at different timepoints. Both fetal CD4⁺ and CD8⁺ T cells upregulated FoxP3 but CD4⁺ T cells appear to express higher levels of both CD25 and FoxP3. **(B)** Representative flow cytometry plots demonstrating the ability of TGFβ to enhance FoxP3 expression by fetal T cells cultured with allogeneic APCs and that inhibition of TGFβ signaling greatly abrogates FoxP3 upregulation (as summarized in Fig. 2E).

Fig. S7

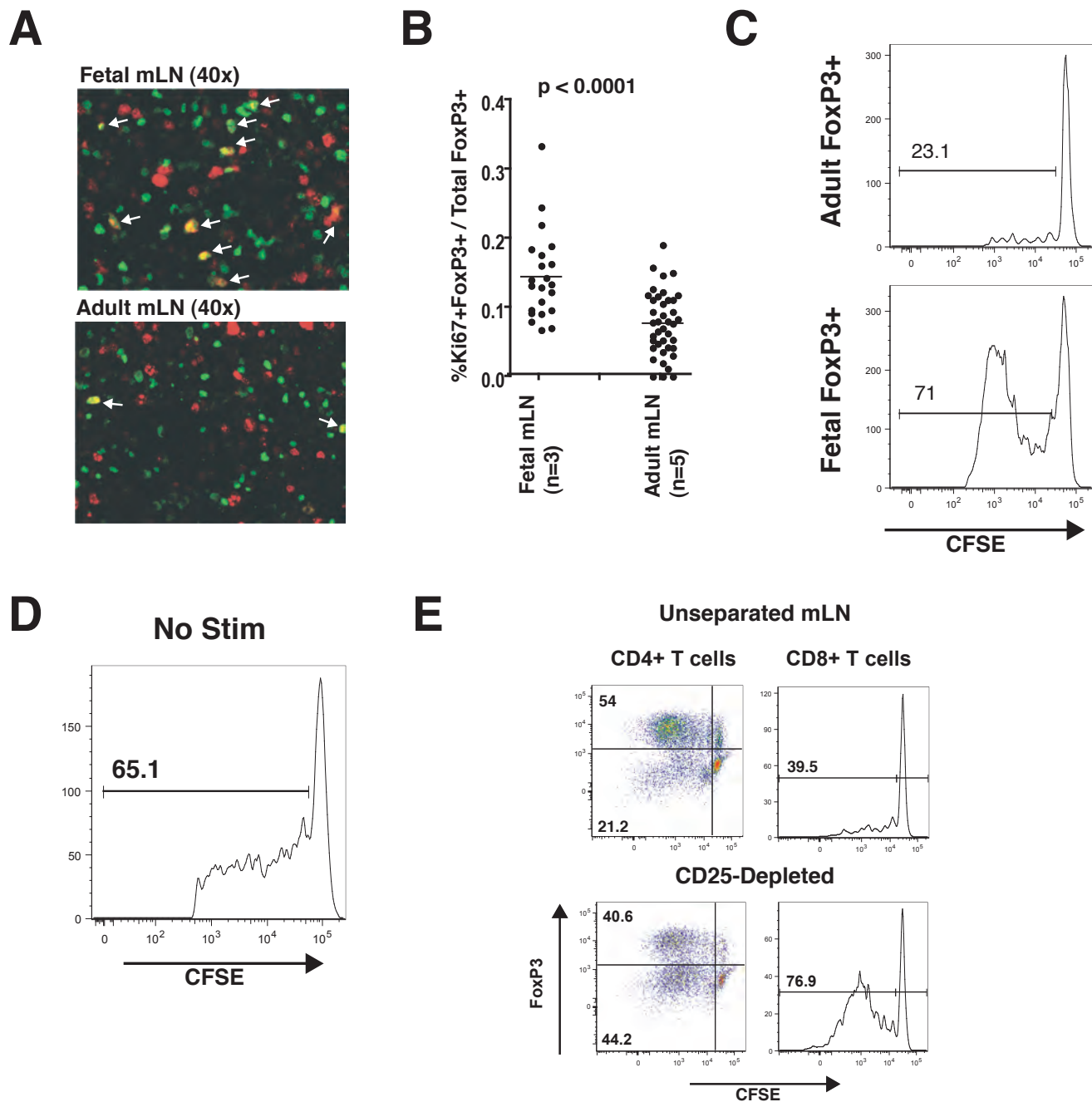


Supplemental figure 7. Acquisition of suppressive properties by fetal T cells following stimulation with unrelated alloantigens *in vitro*. **(A)** Representative purities for fetal mLN CD4⁺CD25⁻ T cells, CD4⁺CD25⁺ (positively selected/depleted T_{Reg}), and splenic CD4⁺CD25⁺ T_{Reg} on day 0. FoxP3 (y-axis) vs CD25 (x-axis) expression is shown. **(B)** Expression of FoxP3 by fetal T cells stimulated for 7 days with unrelated allogeneic APCs with or without addition of TGFβ inhibitor (1 μM) SB-431542. Splenic CD4⁺CD25⁺ T_{Reg} cultured in the presence of 50U/mL IL-2 for 7 days in parallel. Top panels show CD4 vs CD8 expression. Fetal LN cells were depleted of CD8⁺ T cells on day 0 to avoid potential problems with interpreting CFSE dilution by CFSE-labeled CD8⁺ cells responding to alloantigens in add-back assays. **(C)** Individual histograms depicting CFSE-dilution (proliferation) of labeled fetal CD8⁺ splenocytes in add-back suppression assay.



Supplementary figure 8. Additional children-versus-parents MLR data. **(A)** Sort purity after mock depletion (with anti-biotin beads) or depletion of CD25⁺ cells from PBMCs. Typical CD3⁺ T cell fractions are shown for depleted and positively-selected PBMC fractions. Contamination of CD25⁺FoxP3⁻ cells within the positively-selected fraction varied significantly between donors, making add-back suppression assays difficult to interpret. **(B)** Dilutions of autologous, maternal, or paternal APCs for 8-day MLRs. CD4⁺ T cell proliferation was more variable within the lower ranges of allogeneic APCs and had higher background, as determined by autologous MLRs (green lines). CD8⁺ T cell proliferation was more consistent and was therefore chosen as the measure for detecting suppression. The 1:3 dilution was chosen because it provided adequate stimulation to promote CD8⁺ T cell proliferation that was greater than that observed against autologous APCs. **(C)** CD8⁺ T cell proliferation against maternal or paternal APCs using mock-depleted PBMCs as responders. There were no significant differences in the frequency of children's CD8⁺ T cells responding to maternal or paternal APCs in mock depleted ($p=0.22$) or CD25-depleted ($p=0.63$) MLRs. **(D)** Depletion of CD25⁺ T cells does not affect background proliferation observed in autologous MLRs. **(E)** Example of an add-back assay using CD25⁺ cells depicted in panel A, where minimal FoxP3⁻ cells were present. Duplicate assays performed on separate 96-well plates revealed a significant increase in suppression directed against maternal APCs, as compared with paternal APCs, despite no apparent difference in maximal response. **(F)** CD4⁺ T cell proliferation in relation to FoxP3 expression for mock- and CD25 depleted PBMCs. Significant expansion of FoxP3⁺CD4⁺ T cells was observed against autologous, maternal, and paternal APCs. After depletion of FoxP3⁺ T cells, there was a substantial decrease in the frequency of FoxP3^{bright}CD4⁺ T cells. **(G)** Comparison of the number of non-inherited HLA DR and HLA DQ (or both) antigens from mother or father shows that there was a comparable level unshared Class II antigens for both. **(H)** Maternal, but not paternal, CD8⁺ T cell proliferation is increased in response to their children's allogeneic APCs after T_{Reg} removal. Two different ratios of responders:stims are shown (1:3 top, 1:30 bottom).

Fig. S9



Supplemental figure 9. Fetal T_{Reg} cells are actively proliferating *in vivo* and *in vitro*. **(A)** Representative image of fetal mLN (20 g.w.) or adult mLN stained for FoxP3 (green) and the nuclear antigen Ki67 (red) which is upregulated during cellular division. Cells that co-stain for FoxP3 and Ki67 appear yellow. **(B)** Quantification of FoxP3⁺Ki67⁺ cells in relation to total FoxP3⁺ cells in fetal (3 separate donors represented with multiple 40x fields examined) or adult (5 separate donors with >5 40x fields/LN counted) mLN. Fetal mLN had significantly more FoxP3⁺ cells that display signs of active cellular division *in vivo*. Statistical analysis performed by Student's t-test (unpaired). **(C)** Purified adult or fetal CD25⁺ T cells stimulated *in vitro* with unrelated allogeneic APCs for 5 days. Adult CD4⁺FoxP3⁺ T cells were primarily non-responsive whereas fetal CD4⁺FoxP3⁺ T cells were highly responsive. Representative of at least three separate experiments. **(D)** Purified fetal CD25⁺ T cells were isolated from mLN (20 g.w.), labeled with CFSE, and cultured for 5 days with autologous, unlabeled mLN cells. Proliferation of FoxP3⁺ cells was measured by CFSE-dilution. Fetal CD4⁺FoxP3⁺ cells were highly proliferative in the absence of stimulation. **(E)** Representative example fetal T cell responses in the absence of exogenous stimulation (as in Figs. 1B, C, and S3D). The spontaneously proliferating cells are predominantly CD4⁺FoxP3⁺ T_{Reg} cells. Depletion of CD25⁺ cells resulted in the robust expansion of a new population of FoxP3⁺ T cells.